

# Real-Time Monitoring of Glucose Export from Isolated Chloroplasts Using an Organic Electrochemical Transistor

Chiara Diacci, Jee Woong Lee, Per Janson, Gwennaël Dufil, Gábor Méhes, Magnus Berggren,\* Daniel T. Simon, and Eleni Stavrinidou\*

**Biosensors based on organic electrochemical transistors (OECT) are attractive devices for real-time monitoring of biological processes. The direct coupling between the channel of the OECT and the electrolyte enables intimate interfacing with biological environments at the same time bringing signal amplification and fast sensor response times. So far, these devices are mainly applied to mammalian systems; cells or body fluids for the development of diagnostics and various health status monitoring technology. Yet, no direct detection of biomolecules from cells or organelles is reported. Here, an OECT glucose sensor applied to chloroplasts, which are the plant organelles responsible for the light-to-chemical energy conversion of the photosynthesis, is reported. Real-time monitoring of glucose export from chloroplasts in two distinct metabolic phases is demonstrated and the transfer dynamics with a time resolution of 1 min is quantified, thus reaching monitoring dynamics being an order of magnitude better than conventional methods.**

Plants are able to convert energy from sunlight into sugars via the photosynthetic process.<sup>[1]</sup> Chloroplasts are the organelles where the photosynthetic reactions take place, thus representing one of the most abundant natural energy conversion machineries. During the day, plants store excessive photosynthetic products in the form of starch granules in the chloroplasts. During the night, the stored starch is converted

into simpler sugars such as glucose and maltose that are then exported from the chloroplasts to be used for sucrose synthesis in order to supply the plant's energetic demands.<sup>[2]</sup>

The rate of starch degradation and subsequent amount and rate of sugars export from chloroplasts will determine the plant's metabolism, growth, and development during night.<sup>[3]</sup> In addition, it has been shown that the coordination between starch biosynthesis and starch degradation is important for the overall development and productivity of the plant.<sup>[3]</sup> Sugars, apart from being energy sources, are also important signaling molecules related to metabolism, growth, stress responses, and development.<sup>[4]</sup> Conventional methods for monitoring the export of sugars from chloroplasts are complex, labor intensive,

and lack the possibility of real-time monitoring. Most approaches are based on enzymatic assays,<sup>[5–7]</sup> chromatography,<sup>[7]</sup> mass spectrometry,<sup>[8]</sup> or isotopic <sup>14</sup>C labeling.<sup>[9]</sup> These methods hinder real-time kinetic and dynamic *in vitro* studies as it is not possible to directly integrate the biological system to the detector therefore requiring sample collection and preparation. The observation of important physiological events and functions relevant to basic science and agriculture is therefore prevented.

Organic bioelectronic sensors, on the other hand, are ideal for interfacing with biology as they can translate complex biological input to an electronic readout signal. The organic electrochemical transistor (OECT)<sup>[10]</sup> has been extensively used as a biochemical sensor due to its inherent signal transduction and amplification capability, specificity through biofunctionalization, operation at low voltages, robust device design, and easy fabrication, and most importantly its ability to operate in an aqueous environment at high threshold stability. The latter is a fundamental prerequisite for direct coupling with the biological world.<sup>[11–14]</sup> The OECT includes an electrolyte as an integral part of the device configuration that couples the transistor channel with the gate. The sensing mechanism relies on the modulation of the channel current ( $I_{SD}$ ) in the presence of analyte through a reaction that resides either on the gate of the transistor, within the electrolyte or directly on the channel.

So far, most of the OECT-based sensor studies have been focused on developing sensors and diagnostic tools that can be applied in mammalian-related systems, for example, the

C. Diacci, Dr. J. W. Lee, P. Janson, G. Dufil, Dr. G. Méhes, Prof. M. Berggren, Dr. D. T. Simon, Dr. E. Stavrinidou  
Laboratory of Organic Electronics  
Department of Science and Technology  
Linköping University  
601 74 Norrköping, Sweden  
E-mail: magnus.berggren@liu.se; eleni.stavrinidou@liu.se  
Dr. J. W. Lee, Prof. M. Berggren, Dr. E. Stavrinidou  
Wallenberg Wood Science Center  
Department of Science and Technology  
Linköping University  
601 74 Norrköping, Sweden

 The ORCID identification number(s) for the author(s) of this article can be found under <https://doi.org/10.1002/admt.201900262>.

© 2019 The Authors. Published by WILEY-VCH Verlag GmbH & Co. KGaA, Weinheim. This is an open access article under the terms of the Creative Commons Attribution-NonCommercial License, which permits use, distribution and reproduction in any medium, provided the original work is properly cited and is not used for commercial purposes.

The copyright line was changed on 2 August 2019 after initial publication.

DOI: 10.1002/admt.201900262

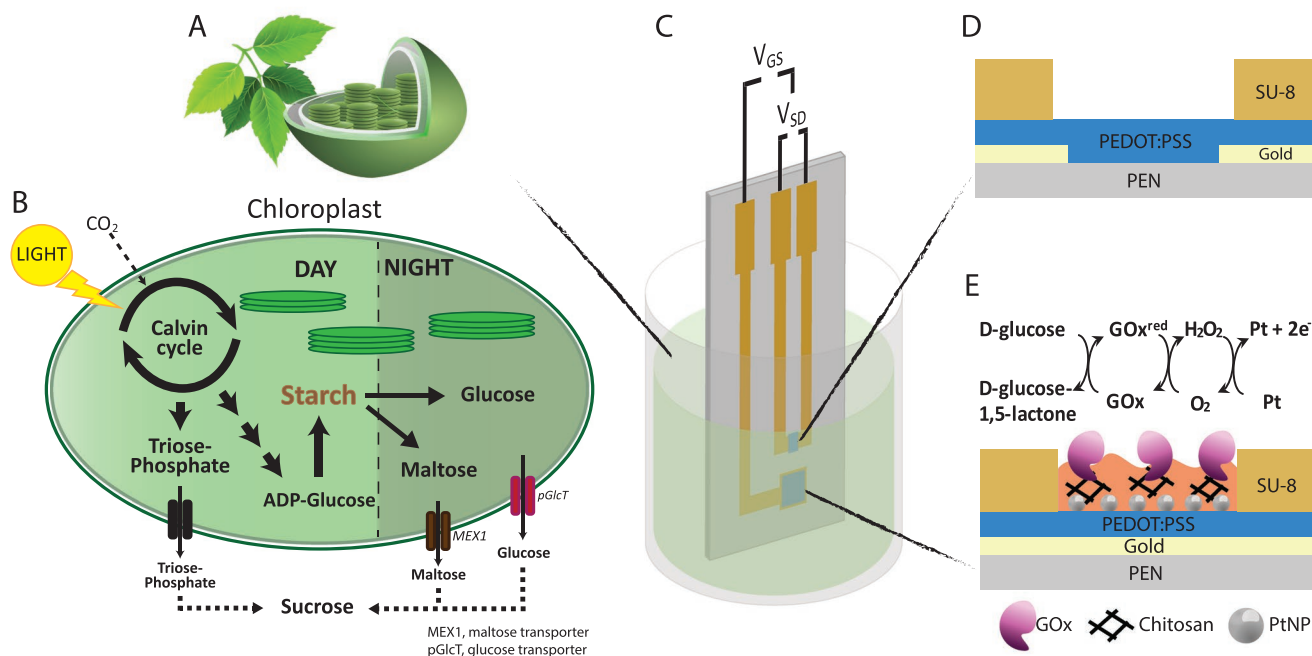


**Figure 1.** Overview of the experimental design for monitoring the export of glucose from isolated chloroplasts using an OECT-based glucose sensor. A) Schematic of chloroplast. B) Chloroplast in starch biosynthesis mode during daytime and starch degradation mode during nighttime. C) OECT setup for detecting glucose in isolated chloroplasts solution. D,E) Structure of OECT channel and gate, functionalized with glucose oxidase.

measurement of pH, detection of ions, metabolites, and neurotransmitters.<sup>[15–22]</sup> Major efforts have been focused on the development of glucose sensors as glucose is one of the most important metabolites and is a crucial parameter and indicator for several diseases. A few demonstrations have been reported where glucose is monitored from natural samples such as sweat,<sup>[21]</sup> saliva,<sup>[20]</sup> or cell media.<sup>[23]</sup> Until now no direct detection of biomolecules from cells or organelles has been reported. In *in vitro* cell studies, for example, the sensor is decoupled from the cell culture and is used as a stand-alone system.<sup>[23,24]</sup>

In this work, for the first time, an OECT-based glucose sensor is directly coupled to isolated chloroplasts, the plant organelles responsible for photosynthesis, for real-time monitoring of glucose export (Figure 1). The OECT is manufactured using standard microfabrication techniques in a planar configuration shaped as a probe-like structure where the gate is biofunctionalized with glucose oxidase (GOx) cross-linked in a chitosan matrix. The chloroplasts are isolated from wild-type tobacco plants, a widely used model system in plant biology, in two distinct metabolic phases, in the starch biosynthesis mode and in the starch degradation mode (Figure 1a,b). We show that glucose is detected only in chloroplasts extracted during nighttime, in agreement with our understanding of the starch degradation process.<sup>[25]</sup> In addition, we demonstrate the kinetics of the glucose export and compare it quantitatively with values previously reported. Our OECT sensor setup and methodology provides a new manner to specifically study metabolic process in chloroplasts, but can be used as a versatile tool by plant biologists to study various kinetic and dynamic processes in plants.

The OECT-based glucose sensor was fabricated with standard thin film and photolithography process protocols. Figure 1 shows the all-planar geometry of the device with channel and gate being

defined on the same substrate. Source, drain, and gate electrodes are based on Au, while the channel consists of a poly(3,4-ethylenedioxythiophene):poly(styrenesulfonate) (PEDOT:PSS) film. The gate is coated with a PEDOT:PSS layer in order to increase its capacitance and ability to fully modulate the channel, and it is further functionalized with platinum nanoparticles (PtNPs) along with the glucose oxidase enzyme. PtNPs are electrodeposited on a chitosan membrane that is previously drop-casted on the gate and has been activated with glutaraldehyde.<sup>[26]</sup> The chitosan provides a desired environment for the enzyme since it is biocompatible, hydrophilic, and it has a high affinity to proteins due to electrostatic interactions. In addition, this immobilization strategy prevents the enzyme from unfolding and also gives the enzyme improved stability against environmental changes.<sup>[27]</sup> When we apply positive gate bias, the channel current decreases as cations from the electrolyte enter the channel and compensate the PSS dopant, thus reducing the overall conductivity of the channel.<sup>[28]</sup> When glucose is present in the solution it will couple to the glucose oxidase enzyme that is immobilized on the gate, and cause a set of redox reactions. D-glucose will be converted to D-glucose-1,5-lactone while the enzyme will be reduced. A product of this reaction, in the presence of oxygen, is hydrogen peroxide, H<sub>2</sub>O<sub>2</sub>, that can be oxidized on the PtNPs on the gate. As electrons are transferred at the gate, the effective gate potential shifts to cause a further decrease of the channel current. This rapid cascade of electrochemical reactions, which was triggered by adding glucose to the electrolyte, is directly coupled to current changes in the OECT, here representing the core principle of glucose sensing of the presented device platform.

To evaluate the basic operation and performance of the developed sensor system, first, we characterized the sensitivity of

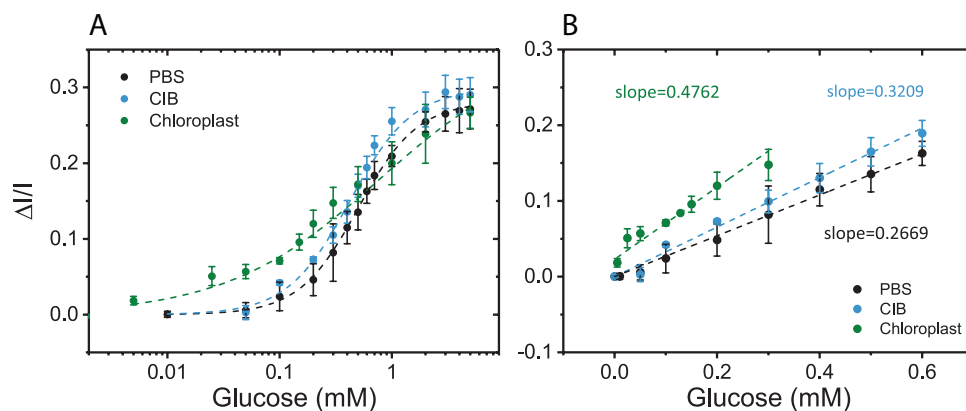


**Figure 2.** Glucose calibration curves of the OECT glucose sensor in different media. A) Normalized response of the OECT functionalized with GOx, to increasing glucose concentrations in PBS buffer (black), CIB buffer (blue), and in inactive chloroplasts solution (green). Dashed lines are fits to sigmoid function. Error bars represent the standard error from three measurements on three different devices. B) Comparison of linear region of glucose calibration curves in different media highlighting the change in sensitivity. Error bars represent the standard error from three measurements on three different devices.

the sensor and performed calibration curves for three different media. The measurements were performed in a phosphate buffer saline (PBS) solution, chloroplast isolation buffer (CIB) solution, and in an inactive isolated chloroplasts solution (CS) to mimic the complex media of the isolated chloroplasts (see **Figure 2**). The sensor was operated using a constant voltage difference applied to the channel,  $V_{SD} = -0.4$  V and gate  $V_{GS} = +0.5$  V. This is an operational regime where the transistor exhibits high transconductance and where  $H_2O_2$  can be oxidized effectively. When no glucose is present in the solution the channel current stabilizes at a certain value. As soon as glucose is added to the solution the current decreases from  $I_0$  to  $I_{gluc}$ . **Figure 2** displays the normalized response ( $NR = -(I_{gluc} - I_0)/I_0$ ) of the sensor versus various glucose concentrations, from  $10 \times 10^{-6}$  to  $5 \times 10^{-3}$  M, in PBS and CIB, respectively. The sensor exhibits a linear response from 10 to  $700 \times 10^{-6}$  and turns saturated at higher concentration of glucose, in the range from  $700 \times 10^{-6}$  to  $5 \times 10^{-3}$  M. Further, since the sensing experiment will be performed in a complex media containing the chloroplasts, we tested the ability of the sensors to operate in such conditions as the physical dimensions of the chloroplast can influence the response and characteristics of the device, in part governed by an increase of the viscosity of the solution or by precipitation effects. Therefore, we calibrated the sensor in a CIB solution, with a known concentration of glucose and nonactive chloroplasts (CS). In this complex media, the device can sense glucose with a corresponding linear regime ranging from 10 to  $300 \times 10^{-6}$ . To ensure that no other interferences arise from the presence of chloroplasts, we used a control device where the enzyme was omitted. Here, no response was observed thus signifying that any recorded change in the output current of the sensors truly originates from changes in glucose concentrations (**Figure S1**, Supporting Information). The full range of the calibration curve was fitted with a sigmoid function that is used to describe processes where dose dependence is observed. **Figure 2B** includes a comparison of the different linear regions of the sensor while operated in different media with corresponding slopes defining the sensitivity of the device. The sensor exhibits higher sensitivity in the chloroplast solution

while compared with operation in buffer solutions, thus manifesting that our sensor device is appropriate to apply in complex media settings.

Having benchmarked the ability of the sensor to operate in complex media, we proceeded to monitor the glucose export from freshly isolated chloroplasts. The chloroplasts were extracted from tobacco plants using a modified isolation protocol<sup>[29,30]</sup> in two distinct metabolic phases, during daytime and during nighttime. The chloroplasts in starch biosynthesis mode are extracted from leaves that are harvested in daytime (typically 6–8 h after the onset of the day cycle) while the chloroplasts that are in the starch degradation mode are harvested during nighttime, at least 2 h after the onset of dark cycle, to ensure that the chloroplasts enter the starch degradation mode but to avoid depletion of the accumulated starch.

Initially, the active areas, including the gate and channel, of the transistor are immersed in the chloroplast isolation buffer solution in a polydimethylsiloxane (PDMS) well as shown in **Figure 1**. The transistor is operated at constant gate potential of  $V_{GS} = +0.5$  V and constant source–drain potential of  $V_{SD} = -0.4$  V until the channel current  $I_{SD}$  is stable. After stabilization, the buffer solution is exchanged with the chloroplast solution. As a control experiment, a transistor without the enzyme but still including the chitosan and nanoparticles is examined and applied to the same chloroplast solution. Therefore, by comparing the current change between control device and the functionalized sensor device, we can extract and quantify the changes in device response due to glucose export from the chloroplasts. In addition, by using a vertical configuration in our setup ensures that there is no interference from precipitated chloroplasts along the active areas of the transistor. All measurements (daytime and nighttime) were performed in darkness to avoid any variation of the current due to light absorption. **Figure 3** displays the typical characteristics of the current response of the OECT sensor when immersed in daytime and nighttime-isolated chloroplasts, in combination with typical response performance of a control device. Chloroplasts in daytime mode do not export any glucose at a measurable concentration as both sensor and control devices have similar response.

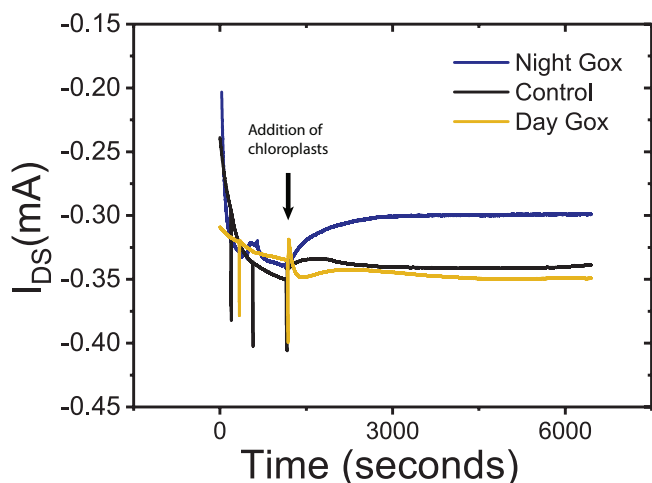


**Figure 3.** Real-time response of OECTs in fresh extracted chloroplast solutions. Typical current response from: control device (without GOx functionalization) in black, GOx-OECT in daytime chloroplasts solution in yellow, and GOx-OECT in nighttime chloroplasts solution in blue.

On the other hand, chloroplasts in the nighttime mode export glucose as seen from the response of the sensor device where the current decreases with time while the control device shows negligible changes. This observation agrees with the current understanding of plant metabolism.<sup>[25]</sup> These results demonstrate that the OECT platform is able to monitor the relevant concentrations of glucose export from active chloroplasts. Based on the calibration curves (Figure 2) we performed a quantitative analysis in order to determine the amount of glucose that is exported from chloroplasts during the nighttime mode.

The characteristics of the exported glucose versus the concentration of intact chloroplasts, for chloroplasts harvested in the nighttime mode, daytime mode, and for the control devices are given in Figure 4. Initially, we observe a fast export of glucose from the nighttime chloroplasts with an increasing trend that lasts for up to 30 min. Then the signal saturates and remains almost constant implying that outflux of glucose from the chloroplasts is smaller than the beginning and that it becomes constant. The absolute glucose concentration in the solution for

the saturation regime is in the range of  $80\text{--}500 \times 10^{-6}$  therefore below the saturation regime of the sensor. We monitor the process for up to 60 min, since this is the time period for which we can ensure that the chloroplasts will remain active. During 1 h, we record an average export of  $170 \text{ nmol glucose mg}^{-1}$  chloroplast. These values agree well with the ones reported in literature for isolated chloroplasts extracted from spinach while measured with traditional enzymatic assays.<sup>[6,7]</sup> Further, with the OECT sensor we are also able to resolve the glucose export dynamics with a resolution of 1 min during the first 10 min. The direct coupling of the chloroplasts with the biosensor allows us to monitor the initial export kinetics at a speed that is not possible with other typical conventional methods, in part due to time lagging that appears from sample preparation.

This reported work is the first example of coupling active plant organelles with a biosensor based on the organic electrochemical transistor. We demonstrate that the OECT sensor can operate in complex media and that it can directly detect the products of the biological unit without any need for additional purification steps or complex sample handling. In addition, the OECT sensor platform is capable to measure the export of glucose in real time, from isolated chloroplasts, with a temporal resolution of 1 min, thus our technology outperforms conventional methods, making it an attractive tool for studying the kinetics of biological processes in general. Further engineering of the device can allow higher temporal resolution with multi-component biochemical sensing.

## Experimental Section

**OECT Fabrication:** A heat-stabilized polyethylene naphthalate (Teonex Q65HA, 125  $\mu\text{m}$ , Peutz Folien GmbH) circular 4 in. substrate was cleaned with acetone and water. Metal films of 2 nm titanium (Ti) and 50 nm gold (Au) were evaporated upon it. Contacts, wiring, channel, and gate(s) are patterned using a Shipley positive resist and photolithography (Karl Suss MA/BM 6 mask aligner), and then wet etched in  $\text{I}_2/\text{KI}$  solution for Au, and  $\text{H}_2\text{O}_2/\text{NH}_4\text{Cl}/\text{H}_2\text{O}$  for Ti. After the substrate was stripped with acetone, a PEDOT:PSS (Clevios PH1000) mixture with 5% v/v EG (ethylene glycol) and 0.5% v/v GOPS (3-glycidyloxypropyl) trimethoxysilane) was spin-coated and patterned using a Shipley positive

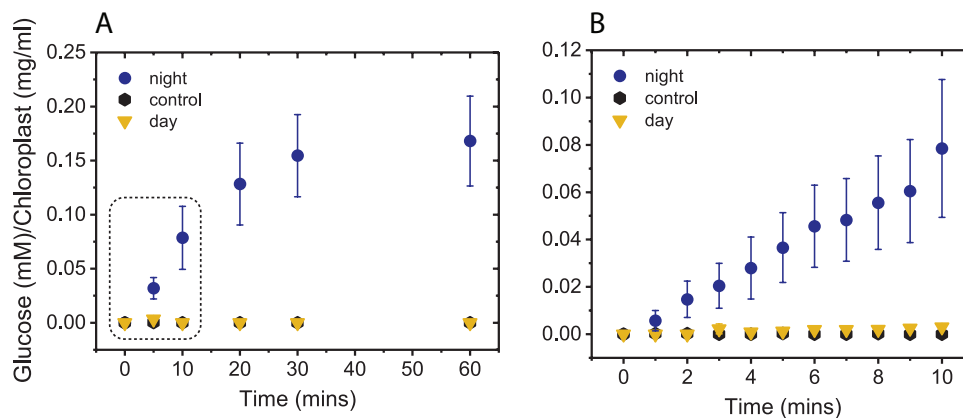


**Figure 4.** Exported glucose per intact chloroplasts concentration as a function of time. A,B) Quantification of glucose export from 0–60 min with 5 min resolution and 0–10 min with 1 min resolution, from nighttime chloroplasts in blue (average of five independent measurements), daytime chloroplasts in yellow (four independent measurements), and control response in black (eight independent measurements).

resist and  $\text{CF}_4/\text{O}_2$  reactive ion etch to define the channel and gate. After another resist strip an ion exchange was made by quickly dipping it into a sodium chloride solution to neutralize the PEDOT:PSS acidity. Finally, the substrate was encapsulated and active areas were defined using SU-8 2010 (MicroChem). Chemicals were used as received from Sigma-Aldrich unless stated otherwise.

**OECT Biofunctionalization:** A  $5 \times 10^{-3} \text{ M}$   $\text{H}_2\text{PtCl}_6$  in aqueous  $50 \times 10^{-3} \text{ M}$   $\text{H}_2\text{SO}_4$  solution was used to deposit Pt nanoparticles on the PEDOT:PSS gate through electrochemical deposition (potentiostat, BioLogic SP-200) using the gate as working electrode, and applying a first fixed potential of +0.7 V for 10 s and a second fixed potential of -0.2 V for 15 s. Enzyme immobilization was performed by drop-casting  $1.5 \mu\text{L}$  of  $0.5 \text{ mg mL}^{-1}$  filtered chitosan (Sigma Aldrich) solution in  $50 \times 10^{-3} \text{ M}$   $\text{CH}_3\text{COOH}$  on the gate electrode. After 30 min the electrode was rinsed with deionized water to remove the remaining  $\text{CH}_3\text{COOH}$ . To crosslink the chitosan,  $1.5 \mu\text{L}$  of glutaraldehyde 2.5 wt% was deposited on top of the membrane for 5 min. As final step  $1.5 \mu\text{L}$  of  $6 \text{ mg mL}^{-1}$  glucose oxidase (Sigma-Aldrich, 100k Units) in PBS (Thermo Fisher) was drop-casted on top of the chitosan membrane and let dry overnight at 4 °C. Then the gate was rinsed and dried gently with a nitrogen stream.

**OECT Characterization and Experimental Setup:** Standard curves in phosphate buffer saline ( $50 \times 10^{-3} \text{ M}$  pH 7.4) and in CIB were performed in a horizontal setup. OECT coupling with active chloroplasts for real-time monitoring experiments and nonactive chloroplasts (extracted chloroplasts from leaves kept in a fridge for several days) and CIB buffer solution 1:1 for standard curves were performed in an inclined setup (see Figure 1) using a PDMS well with a Keithley 2600 series Source Meter. All measurements were carried out at room temperature and real-time measurements were performed in dark. The transistor was operated at constant bias mode with  $V_{\text{SD}} = -0.4 \text{ V}$  and  $V_{\text{SG}} = +0.5 \text{ V}$ . The transistor response was stabilized by exchanging the test solution three times before adding any glucose or the active chloroplasts.

**Plant Materials and Growth Conditions:** The tobacco (wild-type SR1) plants were grown in long-day (16 h light/8 h dark) photoperiodic conditions under white fluorescent light ( $200 \mu\text{mole m}^{-2} \text{ s}^{-1}$ ) at room temperature with 50–60% relative humidity. 8–10 weeks old tobacco plants were used in experiments. For the experiment of glucose dose–response curve in nonactive chloroplasts solution, the chloroplasts were isolated from commercial spinach leaves that were kept in fridge for many days.

**Isolation of Chloroplasts:** Chloroplasts were isolated using the modified protocol of the Sigma Chloroplasts Isolation Kit (Sigma-Aldrich, CP-ISO). All isolation steps were performed at 2–4 °C.  $\approx 30 \text{ g}$  of tobacco leaves were washed with deionized water and the midrib veins were removed and cut into  $\approx 2 \text{ cm}^2$  pieces. Then the pieces were homogenized in a blender (Bosch, ErgoMixx) with 180 mL CIB containing bovine serum albumin (BSA) ( $4 \text{ mL mg}^{-1}$  of leaves) with 5 s strokes. After filtration with a  $100 \mu\text{m}$  nylon mesh, the chloroplasts suspension was centrifuged at  $1000 \times g$  for 7 min. The supernatant was discarded and the remaining green pellet was gently resuspended with 4 mL of  $1 \times$  CIB with BSA by pipette to avoid frothing. Then, the suspension was centrifuged at  $1000 \times g$  for 3 min and the remaining green pellet was gently resuspended with 0.5 mL of  $1 \times$  CIB without BSA by pipette. For the night experiment, the leaves were collected at least 2 h after in the dark while for the day experiments the leaves were collected 6–8 h after the onset of light period. BSA helps to preserve the activity of isolated chloroplasts and refines the separation. In order to evaluate the stability of the isolated chloroplasts, the intactness of freshly isolated chloroplasts left in room temperature over the course of 2 h was measured. The intactness decreased by 4.5% after 30 min, by 5.67% after 60 min, and by 8.29% after 120 min, all values with respect to  $t = 0$ . Freshly extracted chloroplasts were always used in the experiments.

**Measurement of the Concentration and Intactness of Chloroplasts:** The total chlorophyll concentration of chloroplasts was measured to estimate the yield of isolated intact chloroplasts according to Porra et al. method.<sup>[31]</sup>  $10 \mu\text{L}$  of the chloroplast solution was diluted in 5 mL of acetone–deionized (DI) water mixture (80% acetone) and the solution was mixed with vortex. The solution was then centrifuged at  $3000 \times g$

for 5 min. The absorbance of the supernatant was measured at 647 and 664 nm using microplate reader (BioTek, Synergy H1). The reference blank was the acetone–DI water mixture (80% acetone). The chlorophyll concentration was calculated using Equation (1)

$$(\text{g L}^{-1}) = [(17.76 \times A_{647}) + (7.34 \times A_{664})] / 2 \quad (1)$$

The intactness of the isolated chloroplasts was measured using a modified ferricyanide photoreduction method.<sup>[29]</sup> The percentage of intact chloroplasts in the preparation was assessed by comparing the rate of photoreduction of ferricyanide with or without the osmotic shock of chloroplasts. For each of the following reactions, an amount of chloroplasts that is equivalent to  $100 \mu\text{g}$  of chlorophyll was used. To prepare the solution without osmotic shock of chloroplasts (solution A), the chloroplasts were mixed with 4 mL of  $1 \times$  CIB. Then  $60 \mu\text{L}$  of  $100 \times 10^{-3} \text{ M}$  ferricyanide was added. To prepare the solution with osmotic shock of chloroplasts (solution B), the chloroplasts were mixed with 2 mL of DI water. Then incubated for at least 15 s to allow the osmotic shock to take place and then 2 mL of  $2 \times$  CIB and  $60 \mu\text{L}$  of  $100 \times 10^{-3} \text{ M}$  ferricyanide were added. Solution A and B were placed in 96-well plate and absorbance was measured at 410 nm before illumination and after illumination with 46 W white light every 2 min for 8 min. The percent of intact chloroplasts was calculated with Equation (2)

$$\% \text{ intact chloroplasts} = (B - A) / B \times 100 \quad (2)$$

**Data Analysis:** In order to quantify the glucose concentration, the NR was calculated using Equation (3)

$$\text{NR} = -\frac{I_n - I_0}{I_0} \quad (3)$$

where  $I_n$  is the current at the  $n$ th concentration for the standard curve or the current at any given point at the sensing experiment and  $I_0$  is the current at the baseline. The amount of glucose exported by chloroplasts during nighttime and daytime was determined using the chloroplast solution dose–response curve, fitted with a sigmoid function  $y = ax / (b + x)$ , where  $a$  and  $b$  are constants. The amount of glucose from the current was normalized by the amount of intact chloroplasts with Equation (4)

$$\text{Glucose exp} (\text{Mg}^{-1} \text{L}^{-1}) = \frac{\text{Glucose (M)}}{\text{Intact chloroplasts} (\text{g L}^{-1})} \quad (4)$$

where Glucose exp is the amount of glucose exported from chloroplast, glucose (M) is the amount of glucose obtained from the dose–response curve, and Intact chloroplast ( $\text{g L}^{-1}$ ) is the concentration of chloroplasts multiplied by the intactness.

## Supporting Information

Supporting Information is available from the Wiley Online Library or from the author.

## Acknowledgements

C.D., J.W.L., and P.J. contributed equally to this work. The authors wish to thank Åsa Strand, Tamara Hernández-Verdeja, and Totte Niittylä from Umeå Plant Science Center, Benoit Piro from Paris-Diderot University and Xenofon Strakosas from Linköping University for fruitful discussions. Funding was provided by the Knut and Alice Wallenberg Foundation, Linköping University and industry through the Wallenberg Wood Science Center, the Swedish Foundation for Strategic Research (SSF), Vetenskapsrådet (VR), Önnestj Foundation, VINNOVA and the Swedish Government Strategic Research Area in Materials Science on

Functional Materials at Linköping University (Faculty Grant SFO-Mat-LiU No. 2009-00971). Additional funding was provided by the European Union's Horizon 2020 research and innovation programme under Grant Agreement No. 800926 (FET-OPEN-HyPhOE) to E.S. and G.D. and a Marie Skłodowska Curie Individual Fellowship (MSCA-IFEF-ST, Trans-Plant, 702641) to E.S. GM was also supported by a grant from the Swedish MSCA Seal of Excellence program.

## Conflict of Interest

The authors declare no conflict of interest.

## Keywords

chloroplasts, glucose sensing, organic electrochemical transistor, photosynthesis, real-time monitoring

Received: March 27, 2019

Revised: May 9, 2019

Published online:

- [1] J. Soll, E. Schleiff, *Nat. Rev. Mol. Cell Biol.* **2004**, *5*, 198.
- [2] J. Smirnova, A. R. Fernie, M. Steup, *Starch Metab. Struct.* **2015**, *239*.
- [3] A. Graf, A. Schlereth, M. Stitt, A. M. Smith, *Proc. Natl. Acad. Sci. USA* **2010**, *107*, 9458.
- [4] F. Rolland, E. Baena-Gonzalez, J. Sheen, *Annu. Rev. Plant Biol.* **2006**, *57*, 675.
- [5] G. Ritte, K. Raschke, G. Ritte, *New Phytol.* **2003**, 195.
- [6] J. C. Servaites, D. R. Geiger, *J. Exp. Bot.* **2002**, *53*, 1581.
- [7] S. E. Weise, A. P. M. Weber, T. D. Sharkey, *Planta* **2004**, *218*, 474.
- [8] O. Fiehn, J. Kopka, P. Dörmann, T. Altmann, R. N. Trethewey, L. Willmitzer, *Nat. Biotechnol.* **2000**, *18*, 1157.
- [9] M. Stitt, H. W. Heldt, *Plant Physiol.* **1981**, *68*, 755.
- [10] B. D. Nilsson, M. Chen, T. Kugler, T. Remonen, M. Armgarth, M. Berggren, *Adv. Mater.* **2002**, *14*, 51.
- [11] X. Strakosas, M. Bongo, R. M. Owens, *J. Appl. Polym. Sci.* **2015**, *132*, 1.
- [12] J. Rivnay, S. Inal, A. Salleo, R. M. Owens, M. Berggren, G. G. Malliaras, *Nat. Rev. Mater.* **2018**, *3*, 17086.
- [13] G. D. Spyropoulos, J. N. Gelinas, D. Khodagholy, *Sci. Adv.* **2019**, *5*, eaau7378.
- [14] E. Stavrinidou, R. Gabrielsson, E. Gomez, X. Crispin, O. Nilsson, D. T. Simon, M. Berggren, *Sci. Adv.* **2015**, *1*, e1501136.
- [15] F. Mariani, I. Gualandi, M. Tessarolo, B. Fraboni, E. Scavetta, *ACS Appl. Mater. Interfaces* **2018**, *10*, 22474.
- [16] H. Tang, P. Lin, H. L. W. Chan, F. Yan, *Biosens. Bioelectron.* **2011**, *26*, 4559.
- [17] M. Di Lauro, C. Diacci, F. Biscarini, C. A. Bortolotti, V. Beni, M. Berto, D. T. Simon, L. Theuer, M. Berggren, *Flexible Printed Electron.* **2018**, *3*, 024001.
- [18] M. Sessolo, J. Rivnay, E. Bandiello, G. G. Malliaras, H. J. Bolink, *Adv. Mater.* **2014**, 4803.
- [19] L. Kergoat, B. Piro, D. T. Simon, M. C. Pham, V. Noël, M. Berggren, *Adv. Mater.* **2014**, *26*, 5658.
- [20] A. M. Pappa, V. F. Curto, M. Braendlein, X. Strakosas, M. J. Donahue, M. Focchi, G. G. Malliaras, R. M. Owens, *Adv. Healthcare Mater.* **2016**, *5*, 2295.
- [21] A. Aliane, G. Marchand, V. F. Curto, R. Coppard, R. M. Owens, X. Strakosas, G. G. Malliaras, P. Mailley, G. Scheiblin, *MRS Commun.* **2015**, *5*, 507.
- [22] D. J. Macaya, M. Nikolou, S. Takamatsu, J. T. Mabeck, R. M. Owens, G. G. Malliaras, *Sens. Actuators, B* **2007**, *123*, 374.
- [23] X. Strakosas, M. Huerta, M. J. Donahue, A. Hama, A. M. Pappa, M. Ferro, M. Ramuz, J. Rivnay, R. M. Owens, *J. Appl. Polym. Sci.* **2017**, *134*, 1.
- [24] V. F. Curto, B. Marchiori, A. Hama, A. M. Pappa, M. P. Ferro, M. Braendlein, J. Rivnay, M. Focchi, G. G. Malliaras, M. Ramuz, R. M. Owens, *Microsyst. Nanoeng.* **2017**, *3*, 1.
- [25] M. Stitt, S. C. Zeeman, *Curr. Opin. Plant Biol.* **2012**, *15*, 282.
- [26] H. Tang, F. Yan, P. Lin, J. Xu, H. L. W. Chan, *Adv. Funct. Mater.* **2011**, *21*, 2264.
- [27] B. Krajewska, *Enzyme Microb. Technol.* **2004**, *35*, 126.
- [28] E. Stavrinidou, P. Leleux, H. Rajaona, D. Khodagholy, J. Rivnay, M. Lindau, S. Sanaur, G. G. Malliaras, *Adv. Mater.* **2013**, *25*, 4488.
- [29] R. M. C. Lilley, M. P. Fitzgerald, K. G. Rienits, D. A. Walker, *New Phytol.* **1975**, *75*, 1.
- [30] S. P. Robinson, *Photosynth. Res.* **1983**, *4*, 281.
- [31] R. J. Porra, W. A. Thompson, P. E. Kriedemann, *Biochim. Biophys. Acta, Bioenerg.* **1989**, *975*, 384.